

The thermal QCD transition with two flavors of twisted mass fermions

Florian Burger,¹ Ernst-Michael Ilgenfritz,^{1,2} Malik Kirchner,¹ Maria Paola Lombardo,³ Michael Müller-Preussker,¹ Owe Philipsen,⁴ Christopher Pinke,⁴ Carsten Urbach,⁵ and Lars Zeidlewicz⁴

(tmfT collaboration)

¹*Humboldt-Universität zu Berlin, Institut für Physik, 12489 Berlin, Germany*

²*Joint Institute for Nuclear Research, VBLHEP, 141980 Dubna, Russia*

³*Laboratori Nazionali di Frascati, INFN, 100044 Frascati, Roma, Italy*

⁴*Goethe-Universität Frankfurt, Institut für Theoretische Physik, 60438 Frankfurt am Main, Germany*

⁵*Universität Bonn, HISKP and Bethe Center for Theoretical Physics, 53115 Bonn, Germany*

(Dated: December 3, 2012)

We investigate the thermal QCD transition with two flavors of maximally twisted mass fermions for a set of pion masses, $300 \text{ MeV} < m_\pi < 500 \text{ MeV}$, and lattice spacings $a < 0.09 \text{ fm}$. We determine the pseudo-critical temperatures and discuss their extrapolation to the chiral limit using scaling forms for different universality classes, as well as the scaling form for the magnetic equation of state. For all pion masses considered we find reasonable consistency with $O(4)$ scaling plus leading corrections. However, a true distinction between the $O(4)$ scenario and a first order scenario in the chiral limit requires lighter pions than are currently in use in simulations of Wilson fermions.

PACS numbers: 11.15.Ha, 11.10.Wx, 11.30.Rd, 12.38.Gc

Keywords:

I. INTRODUCTION

The transition from a confined phase with broken chiral symmetry to a deconfined chirally symmetric phase is an important subject for studies of finite temperature quantum chromodynamics (QCD). This transition is relevant for the evolution of the early universe and reproduced in current heavy ion collision experiments. It can be investigated non-perturbatively using lattice QCD as long as the chemical potential for fermion number is small, $\mu/T < 1$. A lot of effort has been invested in lattice studies at zero chemical potential, for recent reviews see [1–4]. Impressive progress has been reported very recently by several collaborations working with different fermion discretization schemes [5–10]. In particular, lattice QCD with staggered fermions and physical quark masses does not predict a true phase transition but an analytic crossover in the limit of zero chemical potential [11]. Similarly, results on the transition temperature and the equation of state have predominantly been obtained from simulations with staggered fermions [12–16]. However, this fermion discretization is subject to an on-going debate and there is no formal proof that its continuum limit will reproduce the universality class of QCD [17]. It is therefore desirable to obtain independent results with other discretizations, in order to have some mutual control over systematic errors.

Unfortunately, Wilson-type fermions (and even more so chiral fermion formulations) require higher computational costs. It is thus expedient to study the nature of the phase transition for various larger than physical quark masses and to extrapolate to the physical situation. Moreover, knowing global proper-

ties of the phase transition as a function of the light quark masses constrains the enlarged phase diagram including the strange quark and non-vanishing chemical potential [18]. An as yet unsettled crucial question in this context is the nature of the phase transition in the two-flavor chiral limit. Most studies favor a second order transition in the $O(4)$ universality class [19–24] but there are also claims for a first order transition [25–29]. Since in the continuum and chiral limits the transition is associated with the breaking of a global chiral symmetry, it is necessarily a true and non-analytic phase transition and one of these scenarios has to be realized [30], while an analytic crossover is ruled out. On the other hand, for moderate and intermediate quark masses, the transition is an analytic crossover, before it turns into a first-order deconfinement transition for very heavy quarks.

In this article we study the thermal transition with two degenerate flavors of maximally twisted mass fermions, which provide an $\mathcal{O}(a)$ -improved Wilson fermion discretization, for a review see [31]. As a first step we focus on the determination of the phase boundary, i. e. the pseudo-critical temperatures $T_c(m_\pi)$ using the Polyakov loop, the chiral condensate and the plaquette as observables. We do this for a set of pion masses, $m_\pi \approx 300 - 500 \text{ MeV}$, and attempt various extrapolations to the $N_f = 2$ chiral limit. Similar efforts were recently under way employing clover improved fermions [32–34].

The following section serves to specify our simulation setup. In Section III we introduce the observables and collect the pseudo-critical couplings from our simulations. These results allow for an estimate of the size of the discretization errors present in our simulations. In Section IV we use these pseudo-critical points for an extrapolation to the chiral limit. We discuss pos-

sibilities and limitations in discerning the order of the chiral phase transition. Finally Section V gives some conclusions and an outlook.

II. SIMULATION SETUP

We consider QCD with a mass-degenerate doublet of twisted mass fermions, cf. the review by Shindler [31]. The gauge action is tree-level Symanzik improved while the fermion action is

$$S_F[U, \psi, \bar{\psi}] = \sum_x \bar{\chi}(x) (1 - \kappa D_W[U] + 2i\kappa a \mu_0 \gamma_5 \tau^3) \chi(x). \quad (1)$$

The fermion fields are written in the twisted basis $\{\bar{\chi}, \chi\}$ which is commonly used for numerical simulations. It is connected to the basis of physical fields $\{\bar{\psi}, \psi\}$ for the relevant case of maximal twist via

$$\psi = \frac{1}{\sqrt{2}}(1 + i\gamma_5 \tau^3)\chi \quad \text{and} \quad \bar{\psi} = \bar{\chi} \frac{1}{\sqrt{2}}(1 + i\gamma_5 \tau^3). \quad (2)$$

The quark mass is determined by the hopping parameter κ , which parameterizes the untwisted bare quark mass component,

$$\kappa = (2am_0 + 8r)^{-1}, \quad (3)$$

and the twisted mass parameter μ_0 . The Wilson covariant derivative is given by

$$D_W[U]\psi(x) = \sum_{\mu} ((r - \gamma_{\mu})U_{\mu}(x)\psi(x + \hat{\mu}) + (r + \gamma_{\mu})U_{\mu}^{\dagger}(x - \hat{\mu})\psi(x - \hat{\mu})). \quad (4)$$

In the weak coupling limit, $\beta = 6/g_0^2 \rightarrow \infty$, zero quark mass corresponds to $\kappa = 1/8$, setting $r = 1$. For finite coupling this value of κ gets corrections through mass renormalization. The overall renormalized quark mass M is composed of the twisted and untwisted masses as

$$M^2 = Z_m^2 (m_0 - m_{\text{cr}})^2 + Z_{\mu}^2 \mu_0^2. \quad (5)$$

At maximal twist, the above fermion formulation is automatically $\mathcal{O}(a)$ -improved, i. e. cutoff effects linear in the lattice spacing a are absent for non-zero physical observables. Maximal twist is achieved by tuning the hopping parameter to its critical value κ_c , corresponding to m_{cr} , where the untwisted theory would feature massless pions. The required knowledge of $\kappa_c(\beta)$, as well as other input needed from zero temperature simulations in order to set the scale, can be interpolated from data by the European Twisted Mass Collaboration (ETMC) [35]. In Figs. 1 and 2 we show our interpolations for $\kappa_c(\beta)$ and the lattice spacing $a(\beta)$. Our numerical evaluation proceeds by an HMC algorithm [36] within the publicly available code for QCD with twisted mass fermions [37].

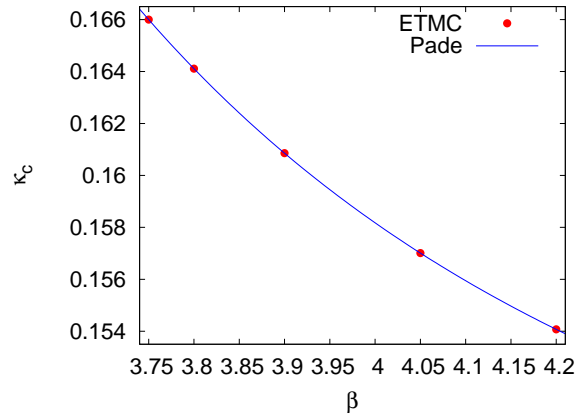


FIG. 1: Interpolation of the critical hopping parameter from ETMC data.

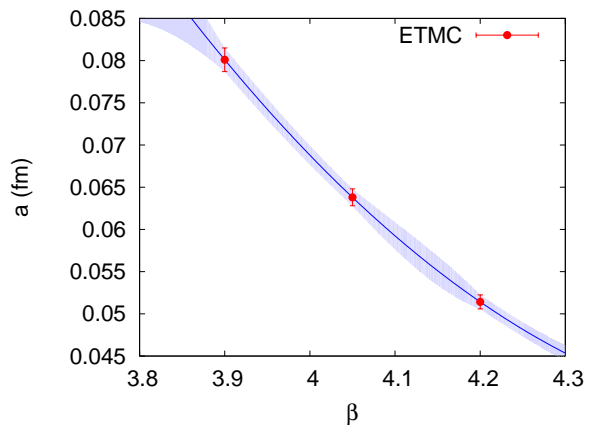


FIG. 2: Interpolation of the lattice spacing from ETMC data.

Wilson fermions are well-known to feature unphysical phases for light quarks and coarse lattice spacings. Like the physical parameter space, these get extended to a third direction because of the additional twisted mass parameter in the current formulation. In order to stay away from unphysical regions, knowledge of the bare parameter phase diagram is required, which we have mapped out earlier in a preparatory study [38]. Status reports of our ongoing project have been given at the annual lattice conferences [39, 40].

The temperature scale is set by the temporal lattice extent and the lattice spacing, $T = 1/(aN_{\tau})$. In order to locate the phase boundary between the hadronic region and the quark gluon plasma, we perform scans in the lattice gauge coupling β , which thus corresponds to a change in temperature of the lattice system. Table I gives the list of runs for different pion masses and the naming scheme that we have adopted for the sake of simplicity. To adjust the masses, ETMC provides parameters for NNLO χ pt-formulae at their values of $\beta \in \{3.8, 3.9, 4.05, 4.2\}$ which can be used to iden-

RUN	$N_\sigma^3 \times N_\tau$	RANGE	m_π (MeV)	$r_0 m_\pi$
A12	$32^3 \times 12$	$3.84 \leq \beta \leq 3.99$	316(16)	0.673(42)
B12	$32^3 \times 12$	$3.86 \leq \beta \leq 4.35$	398(20)	0.847(53)
C12	$32^3 \times 12$	$3.90 \leq \beta \leq 4.07$	469(24)	0.998(62)
B10	$32^3 \times 10$	$3.76 \leq \beta \leq 4.35$	398(20)	0.847(53)

TABLE I: List of scans in β . See also table V.

tify the relation $m_\pi(\mu_0)$ at those couplings. For our $N_\tau = 12$ scans we have relied on the one-loop scaling relation

$$a\mu_0(\beta) = C \exp\left(-\frac{\beta}{12\beta_0}\right), \quad (6)$$

with $\beta_0 = (11 - 2N_f/3)/(4\pi)^2$ and fixing the free parameter C at one of the available couplings. We have found this relation to work sufficiently well to create lines of constant pion mass within the errors quoted in Table I. The run at $N_\tau = 10$ has a constant $a\mu_0 = 0.006$ in the β -interval from 3.865 to 3.930 for which we likewise have the same pion mass within errors in our simulation range. For the other β -values we have adapted the twisted mass according to a two-loop scaling relation similar to the one-loop formula shown above. The free parameter C has been adapted to produce $a\mu_0 = 0.006$ at $\beta = 3.88$.

A final comment concerns the explicit flavor symmetry breaking due to the twisted mass term at finite values of the lattice spacing. This breaking has been investigated by the ETM collaboration for $T = 0$ theoretically [41] and in simulations [35]. The outcome is that effects from flavor breaking – formally of $O(a^2)$ – appear to be negligible in all quantities investigated so far but the neutral pion mass. For this reason we use the charged pion mass throughout the paper. As will be explained in Section IV, for our scaling analysis we need to be close enough to the continuum in order to reproduce chiral symmetry, where flavor breaking should not play any role any longer. Comparison of two lattice spacings appears to justify this assumption. However, a third value of the lattice spacing is required in order to make these statements about the size of lattice artifacts more definite.

III. THERMAL TRANSITION TEMPERATURE

In order to locate the transition, we have used both pure gauge and fermionic observables. The gauge observables are the plaquette

$$P = \frac{1}{6N_c N_\tau N_\sigma^3} \text{ReTr} \sum_x \sum_{\mu > \nu} U_{\mu\nu}(x), \quad (7)$$

with

$$U_{\mu\nu}(x) = U_\mu(x)U_\nu(x + \hat{\mu})U_\mu^\dagger(x + \hat{\nu})U_\nu^\dagger(x), \quad (8)$$

and the real part of the Polyakov loop

$$\text{Re}(L) = \frac{1}{N_c} \frac{1}{N_\sigma^3} \text{ReTr} \sum_{\mathbf{x}} \prod_{x_4=0}^{N_\tau-1} U_4(\mathbf{x}, x_4). \quad (9)$$

The latter is of particular interest since it is the order parameter of the pure gauge deconfinement transition. Along with these observables, we look at their susceptibilities,

$$\chi_O = N_\sigma^3 \left(\langle O^2 \rangle - \langle O \rangle^2 \right). \quad (10)$$

The renormalized (real part of the) Polyakov loop can be determined as [42]

$$\langle \text{Re}(L) \rangle_R = \langle \text{Re}(L) \rangle \exp(V(r_0)/2T), \quad (11)$$

where $V(r_0)$ denotes the static quark-antiquark potential at the distance of the Sommer scale $r = r_0$ [43] to be determined at zero temperature.

The chiral condensate $\langle \bar{\psi}\psi \rangle$ represents the real order parameter of chiral symmetry breaking in the massless limit. An appropriate quantity to locate the chiral phase transition is the chiral susceptibility

$$\chi_\sigma = \frac{\partial \langle \bar{\psi}\psi \rangle}{\partial m_q}. \quad (12)$$

Here, we consider only a part of that expression, the variance per configuration,

$$\sigma_{\bar{\psi}\psi}^2 = V/T \left(\langle (\bar{\psi}\psi)^2 \rangle - \langle \bar{\psi}\psi \rangle^2 \right). \quad (13)$$

This quantity shows a peak associated with the chiral transition. Moreover, it is expected to dominate the signal of χ_σ , see e. g. [44].

The pion norm

$$|\pi|^2 = \sum_x \left\langle \bar{\psi}(x) \frac{1}{2} \gamma_5 \tau^+ \psi(x) \bar{\psi}(0) \frac{1}{2} \gamma_5 \tau^- \psi(0) \right\rangle \quad (14)$$

is interesting for twisted mass simulations because its definition is independent of the fermion basis. It is connected with the chiral condensate via

$$2m_q |\pi|^2 = - \langle \bar{\psi}\psi \rangle, \quad (15)$$

which has been proven for lattice twisted mass fermions in [45]. We have used this relation as a check for $\langle \bar{\psi}\psi \rangle$.

At maximal twist the chiral condensate can be renormalized as follows (see the appendix in [46] and references cited therein)

$$\langle \bar{\psi}\psi \rangle_R = Z_P \langle \bar{\psi}\psi \rangle + c(g_o) \frac{\mu_0}{a^2}. \quad (16)$$

This immediately suggests the form of a subtracted condensate, which is completely standard. However, the subtracted condensate is no longer an order parameter for the chiral transition. It is very easy to fix this problem by adding the zero temperature chiral condensate in the chiral limit. Thus, we introduce a (re)normalized condensate in terms of the ratio

$$R_{\langle\bar{\psi}\psi\rangle} = \frac{\langle\bar{\psi}\psi\rangle(T, \mu_0) - \langle\bar{\psi}\psi\rangle(0, \mu_0) + \langle\bar{\psi}\psi\rangle(0, 0)}{\langle\bar{\psi}\psi\rangle(0, 0)}, \quad (17)$$

where $\langle\bar{\psi}\psi\rangle(T, \mu_0)$ means $\langle\bar{\psi}\psi\rangle$ to be evaluated at non-zero temperature and finite μ_0 . $\langle\bar{\psi}\psi\rangle(0, \mu_0)$ can be obtained from spline interpolations of $T = 0$ $\langle\bar{\psi}\psi\rangle$ data in both the mass μ_0 and β . Additionally, to determine $\langle\bar{\psi}\psi\rangle(0, 0)$ one has to perform a chiral extrapolation of the $T = 0$ $\langle\bar{\psi}\psi\rangle$ data at every β -value one is interested in. We have used a linear extrapolation through three points at every β . The data turned out to be compatible with a linear μ_0 dependence over the whole temperature range we consider here. For the $T = 0$ data we were relying on results provided by the ETM collaboration.

The fermionic observables have been determined using the technique of noisy estimators, as in [47]. For $|\pi|^2$ we have calculated ten propagators per gauge configuration on $Z(2)$ noise vectors. $\langle\bar{\psi}\psi\rangle$ was evaluated using 24 Gaussian volume source vectors for B10, B12 and C12, and 24 $Z(2)$ volume source vectors for A12 respectively. All propagators have been calculated on commodity graphics hardware using NVIDIA's CUDA programming language. The statistics accumulated for the various runs as well as the averages for the Polyakov loop and the chiral condensate are given at the end of the paper in Table V.

Quite generally, we find the signals for the transition to be quite smooth and noisy which presumably is related to the fact that we are merely probing a very soft crossover in our range of pion masses. For a crossover there is no unique definition of a critical temperature as the physics changes smoothly and analytically between the different regions. A pseudo-critical temperature associated with the transition behavior of individual observables is in general observable-dependent.

In Figs. 3 - 6 we show our data for $\sigma_{\bar{\psi}\psi}^2$ in accordance with Eq. (13) and the susceptibility of the real part of the Polyakov loop (Eq. (9)). We quite clearly see maxima for $\sigma_{\bar{\psi}\psi}^2$ in all cases, whereas for the Polyakov loop susceptibility we find only an onset of certain shoulders for the ensembles A12, B12 and B10. At the higher pion mass case C12, where we restricted ourselves to smaller statistics, there seems to appear a maximum also for the Polyakov susceptibility.

In order to estimate the pseudo-critical β_c for chiral transition we have modeled the data for $\sigma_{\bar{\psi}\psi}^2$ with a

RUN	N_τ	β_c	T_χ (MeV)	$r_0 T_\chi$
A12	12	3.89(3)	202(7)	0.437(18)
B12	12	3.93(2)	217(5)	0.473(10)
C12	12	3.97(3)	229(5)	0.500(14)

TABLE II: List of pseudo-critical points for the chiral transition T_χ .

RUN	N_τ	β_c	T_{deconf} (MeV)	$r_0 T_{\text{deconf}}$
B12	12	4.027(14)	249(5)	0.546(13)
C12	12	4.050(15)	258(5)	0.565(14)

TABLE III: List of pseudo-critical points for the deconfinement transition T_{deconf} .

Gaussian

$$c + a \exp\left(-\frac{(\beta - \beta_c)^2}{\sigma^2}\right). \quad (18)$$

The results for the corresponding pseudo-critical chiral transition temperature T_χ are collected in Table II.

In Fig. 7 we show the renormalized chiral condensate ratio $R_{\langle\bar{\psi}\psi\rangle}$ and the renormalized Polyakov loop $\langle\text{Re}(L)\rangle$ for the ensembles B12 and B10. The large error bars for the T -values in case of the B10 ensemble reflect the uncertainty in the scale setting.

By determining the inflection point of the renormalized Polyakov loop $\langle\text{Re}(L)\rangle$ we were able to estimate the deconfinement temperatures T_{deconf} for the ensembles B12 and C12, see Table III.

We clearly see that $T_{\text{deconf}} > T_\chi$ for both higher pion masses. This corresponds to the observation reported in [42].

From weak coupling analyses (valid at high temperature) it is known that the leading order a^2 -scaling towards the continuum limit might not set in before $N_\tau \gtrsim 16$ [48]. Therefore, discretization effects as a major source of systematical errors need to be thoroughly checked. Since the runs B10 and B12 share a common pion mass and differ only by N_τ , they can be used in order to assess the magnitude of cutoff effects. As can be seen from Fig. 6 the quality of $\sigma_{\bar{\psi}\psi}^2$ for the B10 ensemble is not yet precise enough to allow for a Gaussian fit. The available data however suggests a maximum at around $\beta \sim 3.82$ which corresponds to a temperature $T \sim 218$ MeV and agrees with T_χ at $N_\tau = 12$. Moreover the renormalized Polyakov loop and the renormalized chiral condensate (Fig. 7) agree within errors for B10 and B12 indicating small cutoff effects.

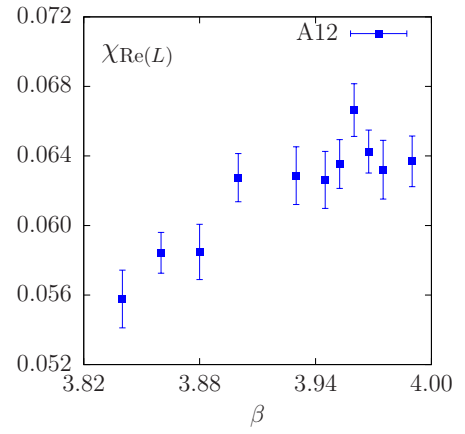
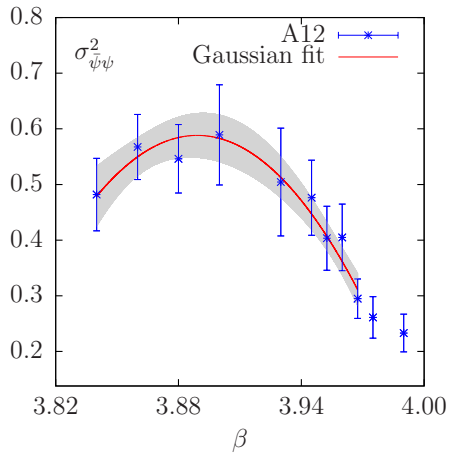


FIG. 3: $\sigma_{\psi\psi}^2$ (left) and susceptibility of $\text{Re}(L)$ (right), both for run A12.

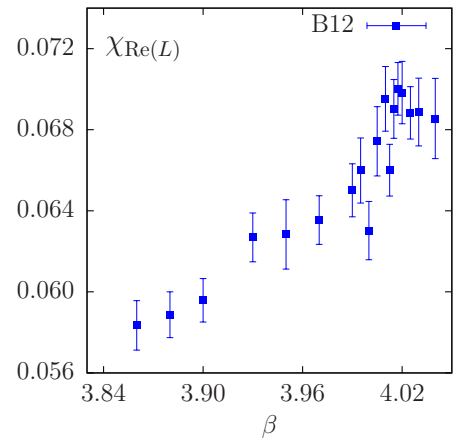
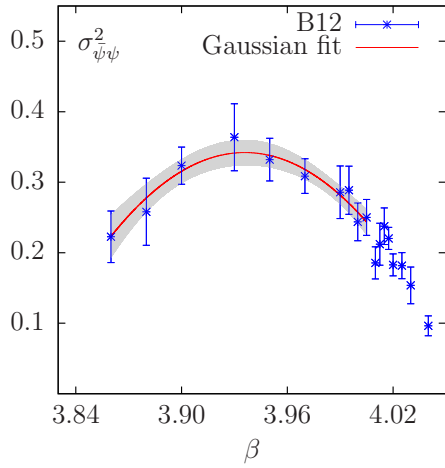


FIG. 4: $\sigma_{\psi\psi}^2$ (left) and susceptibility of $\text{Re}(L)$ (right), both for run B12.

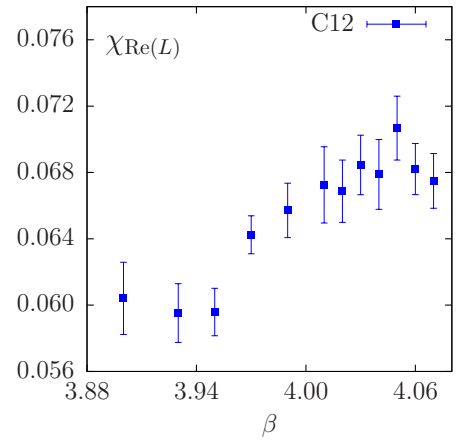
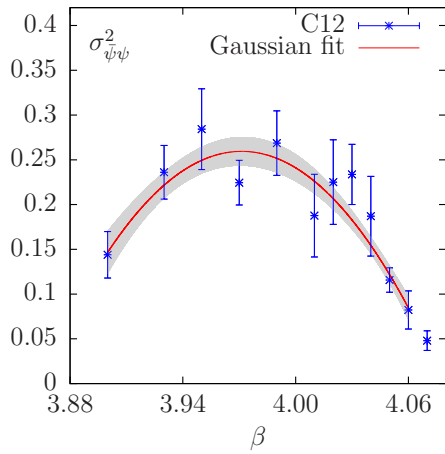


FIG. 5: $\sigma_{\psi\psi}^2$ (left) and susceptibility of $\text{Re}(L)$ (right), both for run C12.

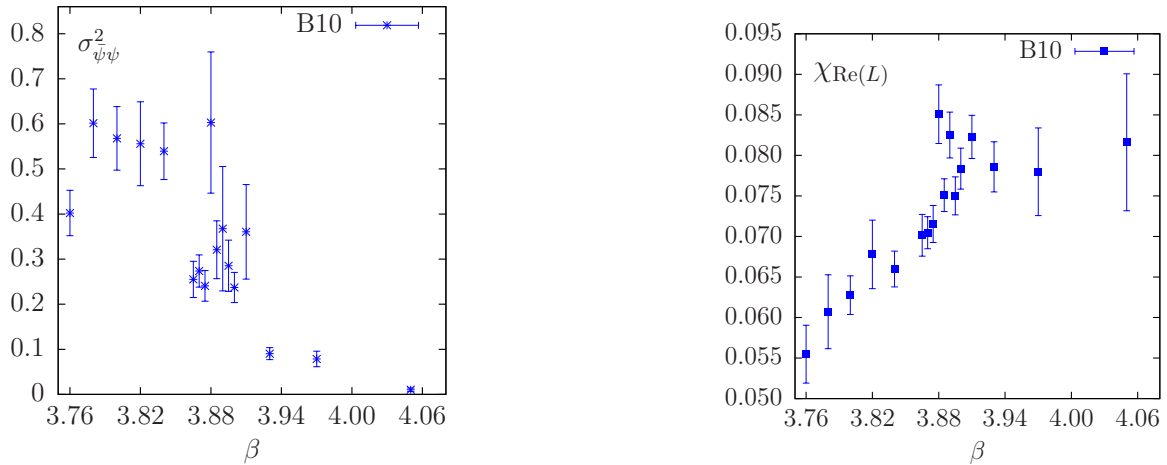


FIG. 6: $\sigma_{\psi\psi}^2$ (left) and susceptibility of $\text{Re}(L)$ (right), both for run B10.

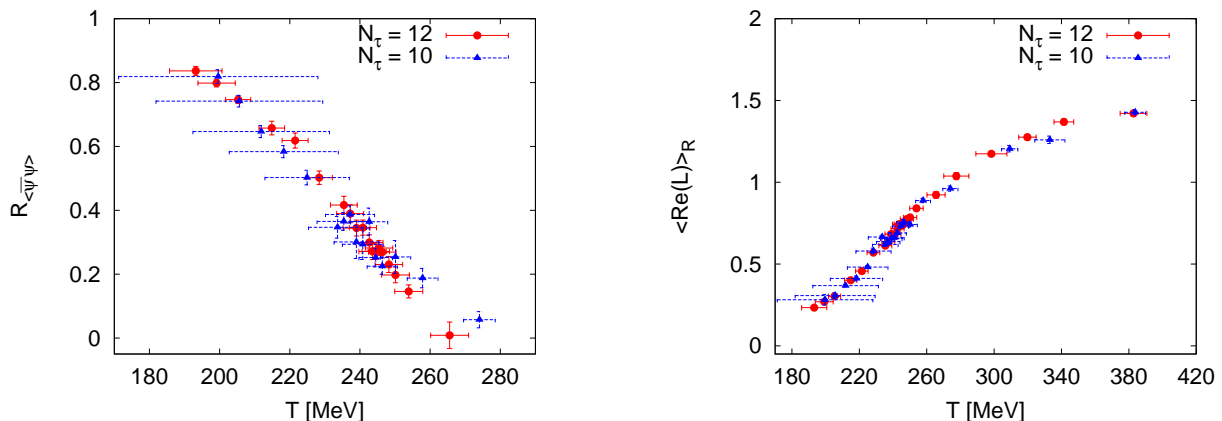


FIG. 7: Ratio $R_{\langle\bar{\psi}\psi\rangle}$ acc. to Eq. (17) (left) and renormalized Polyakov loop $\langle\text{Re}(L)\rangle_R$ (right), both for runs B12 and B10.

IV. TOWARDS THE CHIRAL LIMIT

As indicated in the Introduction, the main interest in the $N_f = 2$ thermal transition lies in its chiral limit, for which one would like to unequivocally determine the order of the phase transition. The chiral condensate $\langle\bar{\psi}\psi\rangle$ then is an order parameter corresponding to the magnetization in an appropriate spin model of the same universality class. Finite quark (and therefore pion) masses break the chiral symmetry explicitly, thus corresponding to an external field. Provided the $N_f = 2$ chiral limit features a second order transition and belongs to the $O(4)$ universality class, one may extrapolate finite mass simulations using universal scaling relations, which hold within some scaling region around the critical phase transition [19, 21]. A priori it is not known how far into the massive region scaling extends, i.e. one can merely test consistency of the data with scaling. A further difficulty is that chiral symmetry is broken explicitly

for Wilson fermions at finite lattice spacing, even in the massless case. Any universal behavior for these types of fermions thus corresponds to continuum scaling, which can only be observed once discretization errors are sufficiently small. Finally, the scaling relations we employ here are valid in the thermodynamic limit. Dedicated finite-size scaling analyses are required to establish the appropriate lattice sizes, but this is beyond the scope of the present study. Again, we assume our lattices to be sufficiently large and test for consistency with scaling.

We begin by attempting a fit of $T_\chi(m_\pi)$ to the scaling form [21, 49]

$$T_\chi(m_\pi) = T_\chi(0) + A \cdot m_\pi^{2/(\tilde{\beta}\delta)}, \quad (19)$$

where we have dressed the critical exponent $\tilde{\beta}$ with a tilde in order to distinguish it from the lattice coupling. The “external field” in this case is the quark mass specified by the mass parameter $a\mu_0$, which in turn is connected to the pion mass in LO χ pt via

$m_\pi^2 \sim \mu_0$. Thus, it is important to keep the pion mass small for two reasons, the validity of both the scaling window and the LO of χ pt. While there is good reason to expect that our pion masses are sufficiently small for the latter [35], the size of the scaling region remains unknown at present. Unfortunately, we do not have sufficiently many data points or sufficiently small errors in order to determine the exponents, but fix the exponents and fit A and $T_c(0)$ only. For $O(4)$ we have $2/(\tilde{\beta}\delta) = 1.08$ and the resulting extrapolation is shown in Fig. 8, giving a chiral critical temperature $T_\chi(m_\pi = 0) = 152(26)$ MeV. It is now interesting to ask whether $O(4)$ scaling can be discriminated from other behavior. As discussed earlier, the alternative scenario is a first order phase transition in the chiral limit. Often in the literature the same scaling relation is tested by merely changing to “first order exponents” ($2/(\tilde{\beta}\delta) = 2$) [14, 50]. Doing so leads to an extrapolation with somewhat larger $T_\chi(m_\pi = 0) = 182(14)$ MeV. However, it is unclear to us whether the scaling relation is applicable in this case. Firstly, for a first order phase transition there is no diverging correlation length. Approaching T_χ in the infinite-volume limit from above and below proceeds in different phases, with finite correlation length in each. Hence, there is no scaling and no universality in the sense of second order transitions (in particular $\tilde{\beta} = 0$ and $\delta = \infty$ separately). The “critical exponents” usually associated with first order transitions specify the approach of the thermodynamic limit in finite-size scaling analyses, but do not apply to the relation (19) in the thermodynamic limit (for a detailed discussion of scaling for first order phase transitions, see [51]). Secondly, if the chiral limit indeed features a first order phase transition, it will weaken with finite quark masses until it vanishes in a $Z(2)$ critical endpoint. Fig. 9 shows the two possible scenarios. However, this means that coming from the crossover region at larger quark masses, an extrapolation to the chiral limit is never exact, as it would pass through a singularity at the critical point. Rather, the approach of this singularity will again be characterized by scaling, this time in the $Z(2)$ universality class. In this case we may use again the relation (19), but with a finite critical pion mass marking the critical point, $m_\pi^2 \rightarrow (m_\pi^2 - m_{\pi,c}^2)$. We have attempted such extrapolations also. Our data are not sufficient to constrain $m_{\pi,c}$. Therefore, Fig. 8 shows two extrapolations, one with $m_{\pi,c} \approx 0$ and another with $m_{\pi,c} \approx 200$ MeV. As the figure illustrates, our extrapolations alone cannot yet discriminate between the first order and second order scenarios. This would require drastically smaller pion masses, lower than the physical value even. Nevertheless, utilising knowledge about T_c from other simulations we still obtain a tendency. The fit assuming a first order scenario leads to a critical temperature which is somewhat larger than expected from other investigations [1]. Of course, those extrapolations are

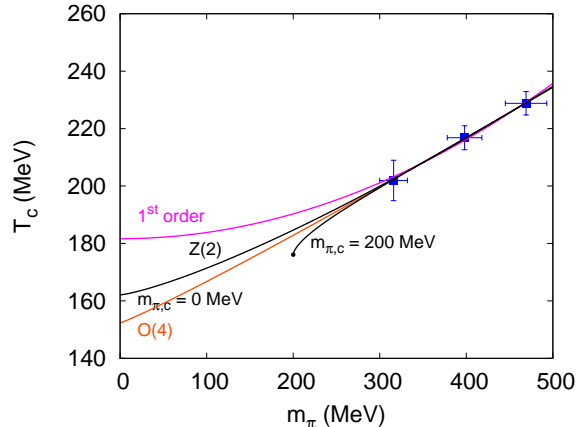


FIG. 8: Chiral extrapolation for $T_\chi(m_\pi)$ for various scenarios as explained in the text.

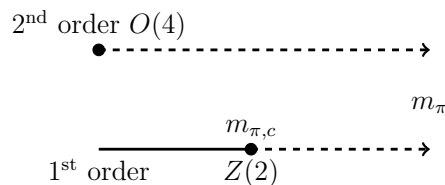


FIG. 9: Illustration of possible scenarios for the $N_f = 2$ chiral limit.

likewise valid only in the $O(4)$ scenario, so again this is merely a consistency test.

For a fixed N_τ , assumed to be large enough so as to be sufficiently close to the continuum, it is also possible to obtain the chiral critical β by means of the scaling relation [21, 49]

$$\beta_c(h) = \beta_{\text{chiral}} + B \cdot h^{1/(\tilde{\beta}\delta)}, \quad h = 2a\mu_0 \quad (20)$$

with $1/(\tilde{\beta}\delta) = 0.537$ corresponding to $O(4)$ exponents. For $N_\tau = 12$ our estimates for β_c are shown in Fig. 10 and can be extrapolated in this manner.

Consistent fits have been found taking all three points from A12 to C12 into account. The result for the critical chiral β -value is

$$\beta_{\text{chiral}}(N_\tau = 12) = 3.73(9). \quad (21)$$

We have carried out the same fit but with the two lower pion mass values (A12 and B12) only. It ended up with the same value. This result corresponds to $T_\chi(m_\pi = 0) \approx 152(26)$ MeV where the error results from the scale setting. This number is in accord with our fits for $T_\chi(m_\pi)$ for a second order transition in the chiral limit. Note however, that the lattice spacing necessary to set the scale stems from an extrapolation to smaller values of β than available from ETMC. This is reflected in the large uncertainty assigned to the temperatures.

Next, the scaling of the magnetic equation of state can be investigated, Fig. 11, where we follow previous

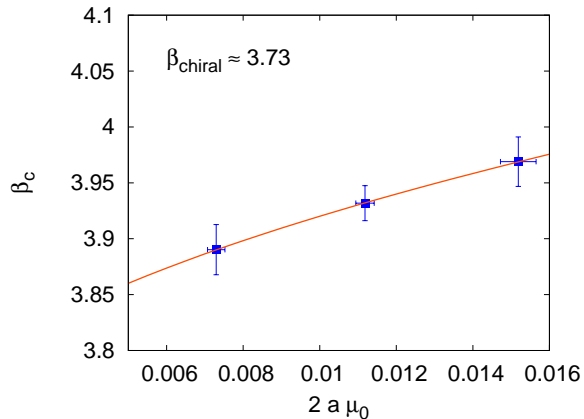


FIG. 10: Critical couplings β_c as function of the external field h .

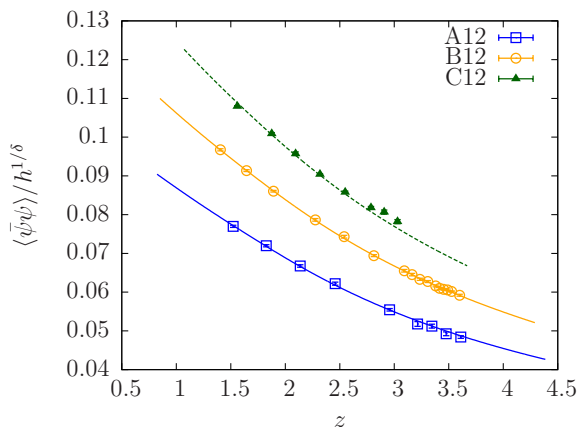


FIG. 11: Scaling for the bare $\langle \bar{\psi}\psi \rangle$ data at $N_\tau = 12$ as function of the scaling variable with modelling of scaling violations. The fit shown is for the combined A12 and B12 data (fit No 10 in Table IV).

studies [21, 24]

$$\langle \bar{\psi}\psi \rangle = h^{1/\delta} c f(d \tau / h^{1/(\tilde{\beta}\delta)}), \quad (22)$$

with

$$\tau = \beta - \beta_{\text{chiral}}. \quad (23)$$

The functional form of the scaling function f for the $O(4)$ case is known [52, 53]. Since we do not know the correct normalization for τ and h with respect to QCD, we are left with two free parameters, c and d , that have to be fitted. We perform the fits in the β -intervals from $\beta = 3.83(3.85, 3.89)$ to $\beta = 3.97(4.03, 4.04)$ for A12 (B12, C12), respectively. The fit results are collected in Table IV.

A fit for the line A12 works quite well, $\chi^2/\text{dof} = 0.43$, but giving $\beta_{\text{chiral}} = 3.57(4)$, which is smaller than the value estimated above by applying eq. (20). In general we observe an increase of χ^2 and a decrease

of β_{chiral} with increasing mass. Indeed, B12 yields $\beta_{\text{chiral}} = 3.40(5)$, which would correspond to a much too low critical temperature below 100 MeV, while C12 gives even smaller values with larger χ^2 . Thus, the fit seems to account for scaling violations due to large mass by decreasing β_{chiral} .

However, scaling violations due to the quark mass can be taken into account by an ansatz including corrections [24],

$$\langle \bar{\psi}\psi \rangle = h^{1/\delta} c f(d \tau / h^{1/(\tilde{\beta}\delta)}) + a_t \tau h + b_1 h + b_3 h^3 + \dots \quad (24)$$

We have fitted our data in numerous ways by taking into account one, two or even three violation terms. Joint fits to the A12 + B12 ensembles are feasible in all three combinations, giving a β_{chiral} the more consistent with the previous determination the more violation terms are included (see Table IV). In Fig. 11 we show a combined fit to A12 and B12 fixing $\beta_{\text{chiral}} = 3.73$ from our independent determination with $\chi^2/\text{dof} = 0.63$. Note that these fits with the two lower order violation terms are not able to include the C12 data with the requirement of a reasonable value of χ^2/dof . However, if we include the next higher violation term $b_3 h^3$ in the combined fit to A12, B12 and C12 we obtain an acceptable $\chi^2/\text{dof} = 1.8$, see the last line of Table IV. We observe that in this case the fit even prefers a value for β_{chiral} compatible with the one from the analysis based on eq. (20).

Since we are in a range of the scaling variable $\tau / h^{1/(\tilde{\beta}\delta)}$ where the scaling function is rather flat, judgement on whether there are additional violations of the $O(4)$ behavior or not is difficult. Repeating this exercise for the first order scenario with endpoint does not give further insight as the combinations of exponents are very close, $1/(\tilde{\beta}\delta) = 0.537, 0.638$ and $1/\delta = 0.21, 0.20$ for $O(4)$ and $Z(2)$, respectively. Therefore, our data are consistent with the $O(4)$ scenario, but do not rule out the possibility of the first order case. This would require drastically smaller pion masses combined with finite-size studies, as the window for chiral scaling appears to set in for $m_\pi \ll 300$ MeV.

V. CONCLUSIONS

We have presented a (revised) first investigation of the two-flavor thermal QCD transition with maximally twisted mass fermions. Our results are compatible with existing work although, of course, staggered investigations are much more advanced [12, 13, 15, 54]. The quality of our signals is comparable to recent results with clover improved Wilson fermions [33, 50].

For three pion masses in the range $300 \text{ MeV} < m_\pi < 500 \text{ MeV}$ we have determined pseudo-critical temperatures for the crossover from the hadronic regime to the quark gluon plasma. The pseudo-critical

No	DATA	β_{chiral}	c	d	a_t	b_1	b_3	χ^2/dof
1	A12	3.57(4)	0.14(2)	0.367(7)	0	0	0	0.43
2	B12	3.40(5)	0.22(4)	0.36(2)	0	0	0	0.64
3	C12	3.12(2)	0.42(3)	0.39(2)	0	0	0	2.42
4	A12 + B12	3.368(6)	0.257(6)	0.383(5)	0	0	0	3.31
5	A12 + B12	3.48(2)	0.225(6)	0.48(2)	0.7(1)	0	0	2.2
6	A12 + B12	3.57(2)	0.152(7)	0.53(2)	0	0.90(6)	0	1.75
7	A12 + B12	3.82(4)	0.028(9)	1.1(2)	-2.2(2)	2.49(8)	0	0.42
8	A12 + B12	3.73	0.1279(8)	0.825(8)	4.01(4)	0	0	76
9	A12 + B12	3.73	0.0759(7)	0.81(2)	0	1.61(2)	0	7.2
10	A12 + B12	3.73	0.053(2)	0.74(2)	-1.8(2)	2.23(6)	0	0.63
11	A12 + B12 + C12	3.76(2)	0.047(6)	0.83(6)	-1.5(2)	2.20(6)	50(11)	1.8

TABLE IV: Fit results based on eq. (24) for several combinations of our data sets and fit parameters. Numbers in bold face have been fixed before fitting. The fit shown in Fig. 11 corresponds to line No 10.

temperatures - extracted for the two higher mass values - from observables related to chiral and deconfinement transitions, respectively, turned out to be different. Discretization effects in T_c appeared to be small for our lattice spacings, $a < 0.09$ fm.

We have restricted ourselves to pion masses < 500 MeV in order to assure the validity of LO χ pt as well as the scaling forms in order to extrapolate to the chiral limit. Assuming the scaling forms appropriate for different universality classes, such extrapolations gave critical temperatures in the range $T_c \sim 140 - 200$ MeV consistent with other studies. However, detailed fitting analyses demonstrated that the second order $O(4)$ scaling regime is not yet reached. Scaling violations could be accommodated by leading order corrections due to finite-mass effects up to $m_\pi \sim 400$ MeV, while heavier masses violate even those corrections. By including higher order violation effects reasonable fits could be achieved with β_c values consistent with the other determinations.

We find that truly distinguishing between the dif-

ferent universality classes and thus ruling out a first order scenario will require much smaller pion masses, $m_\pi \lesssim m_\pi^{\text{phys}}$ as well as finite-size scaling analyses. We hope to address these issues in future investigations.

Acknowledgments

We express our gratitude to Giancarlo Rossi for clarifying the issue of renormalization in the twisted mass case. Moreover, M.P.L. and L.Z. thank Roberto Frezzotti for useful discussions. O.P. and L.Z. are supported by DFG grant PH 158/3-1, C.P. by the German BMBF grant 06FY7100. F.B. and M.M.P. acknowledge support by DFG GK 1504 and SFB/TR 9, respectively. We are grateful to the HLRN supercomputing centers Berlin and Hannover and apeNext in Rome as well as the LOEWE-CSC in Frankfurt for computing resources.

-
- [1] K. Kanaya, PoS **Lat2010**, 012 (2010), 1012.4247.
 - [2] L. Levkova, PoS **LATTICE2011**, 011 (2011), 1201.1516.
 - [3] O. Philipsen (2012), 1207.5999.
 - [4] M. P. Lombardo, Plenary talk given at Lattice 2012, to appear in PoS **LATTICE2012** (2012).
 - [5] A. Bazavov et al. (HotQCD Collaboration), Phys.Rev. **D86**, 034509 (2012), 1203.0784.
 - [6] A. Bazavov et al. (HotQCD Collaboration) (2012), 1205.3535.
 - [7] S. Borsanyi, Y. Delgado, S. Dürer, Z. Fodor, S. Katz, S. Krieg, T. Lippert, D. Negradi, and K. Szabo, Phys.Lett. **B713**, 342 (2012), 1204.4089.
 - [8] S. Borsanyi, S. Dürer, Z. Fodor, C. Hoelbling, S. Katz, S. Krieg, D. Negradi, K. Szabo, B. Toth, and N. Trombitas, JHEP **1208**, 126 (2012), 1205.0440.
 - [9] T. Umeda et al. (WHOT-QCD Collaboration), Phys.Rev. **D85**, 094508 (2012), 1202.4719.
 - [10] S. Ejiri, K. Kanaya, and T. Umeda (WHOT-QCD Collaboration) (2012), 1205.5347.
 - [11] Y. Aoki, G. Endrodi, Z. Fodor, S. Katz, and K. Szabo, Nature **443**, 675 (2006), hep-lat/0611014.
 - [12] S. Borsanyi et al. (Wuppertal-Budapest), JHEP **09**, 073 (2010), 1005.3508.
 - [13] S. Borsanyi et al., JHEP **11**, 077 (2010), 1007.2580.
 - [14] M. Cheng et al., Phys. Rev. **D74**, 054507 (2006), hep-lat/0608013.
 - [15] M. Cheng et al., Phys. Rev. **D81**, 054504 (2010), 0911.2215.
 - [16] A. Bazavov, T. Bhattacharya, M. Cheng, C. De-

A12				
β	T [MeV]	STAT	$\text{Re}(L)$	$\langle \bar{\psi}\psi \rangle$
3.8400	187(10)	3471	$6.1(4) \cdot 10^{-4}$	0.0284(1)
3.8600	193(8)	7114	$6.7(3) \cdot 10^{-4}$	0.0264(1)
3.8800	199(6)	3891	$8.8(4) \cdot 10^{-4}$	0.0243(1)
3.9000	205(4)	6666	$9.8(4) \cdot 10^{-4}$	0.0225(2)
3.9300	215(4)	3947	$1.40(4) \cdot 10^{-3}$	0.0199(1)
3.9450	220(4)	4839	$1.60(5) \cdot 10^{-3}$	0.0185(2)
3.9525	222(4)	5962	$1.67(4) \cdot 10^{-3}$	0.0183(2)
3.9600	225(4)	6112	$1.86(5) \cdot 10^{-3}$	0.0176(2)
3.9675	228(4)	7112	$1.98(5) \cdot 10^{-3}$	0.0172(2)
3.9750	230(4)	4505	$2.06(6) \cdot 10^{-3}$	0.0168(2)
3.9900	235(4)	4796	$2.45(5) \cdot 10^{-3}$	0.0158(2)

B12				
β	T [MeV]	STAT	$\text{Re}(L)$	$\langle \bar{\psi}\psi \rangle$
3.8600	193(8)	7198	$5.95(22) \cdot 10^{-4}$	0.03916(12)
3.8800	199(6)	7883	$7.29(22) \cdot 10^{-4}$	0.03677(10)
3.9000	205(4)	9568	$8.67(19) \cdot 10^{-4}$	0.03444(09)
3.9300	215(4)	9204	$1.24(03) \cdot 10^{-3}$	0.03122(13)
3.9500	222(4)	4788	$1.49(05) \cdot 10^{-3}$	0.02932(14)
3.9700	228(4)	8387	$1.96(07) \cdot 10^{-3}$	0.02724(10)
3.9900	235(4)	8968	$2.09(05) \cdot 10^{-3}$	0.02557(13)
3.9950	237(4)	6486	$2.31(04) \cdot 10^{-3}$	0.02515(13)
4.0000	239(4)	6298	$2.51(04) \cdot 10^{-3}$	0.02464(11)
4.0050	241(4)	7353	$2.54(05) \cdot 10^{-3}$	0.02438(10)
4.0100	243(4)	6403	$2.70(05) \cdot 10^{-3}$	0.02391(10)
4.0125	244(4)	10139	$2.81(04) \cdot 10^{-3}$	0.02365(11)
4.0150	245(4)	8950	$2.84(04) \cdot 10^{-3}$	0.02353(10)
4.0175	245(4)	11673	$2.82(03) \cdot 10^{-3}$	0.02346(09)
4.0200	246(4)	10003	$2.88(04) \cdot 10^{-3}$	0.02328(07)
4.0250	248(4)	9878	$3.02(04) \cdot 10^{-3}$	0.02288(10)
4.0300	250(4)	5245	$3.14(05) \cdot 10^{-3}$	0.02251(09)
4.0400	254(4)	5350	$3.43(05) \cdot 10^{-3}$	0.02186(07)
4.0700	266(6)	1024	$4.00(08) \cdot 10^{-3}$	0.02025(10)
4.1000	278(8)	7837	$4.83(09) \cdot 10^{-3}$	0.01894(04)
4.1500	298(10)	4080	$6.17(07) \cdot 10^{-3}$	0.01736(03)
4.2000	320(6)	4160	$7.57(08) \cdot 10^{-3}$	0.01583(02)
4.2500	341(6)	4160	$9.17(07) \cdot 10^{-3}$	0.01451(03)
4.3500	383(8)	4334	$1.21(01) \cdot 10^{-2}$	0.01185(01)

C12				
β	T [MeV]	STAT	$\text{Re}(L)$	$\langle \bar{\psi}\psi \rangle$
3.9000	205(4)	3050	$8.4(5) \cdot 10^{-4}$	0.0465(2)
3.9300	215(4)	3101	$1.16(4) \cdot 10^{-3}$	0.0431(2)
3.9500	222(4)	5822	$1.35(3) \cdot 10^{-3}$	0.0407(2)
3.9700	228(4)	9179	$1.63(3) \cdot 10^{-3}$	0.0379(2)
3.9900	235(4)	5151	$2.11(5) \cdot 10^{-3}$	0.0360(2)
4.0100	242(4)	4640+5432	$2.48(5) \cdot 10^{-3}$	0.0341(2)
4.0200	246(4)	5120+3324	$2.49(6) \cdot 10^{-3}$	0.0336(3)
4.0300	250(4)	6240+3308	$2.92(7) \cdot 10^{-3}$	0.0325(3)
4.0400	254(4)	4080+3308	$3.20(7) \cdot 10^{-3}$	0.0315(3)
4.0500	258(5)	4640	$3.57(8) \cdot 10^{-3}$	0.0306(2)
4.0600	262(5)	5523	$3.79(5) \cdot 10^{-3}$	0.0296(1)
4.0700	266(6)	2790	$4.20(5) \cdot 10^{-3}$	0.0288(1)

B10				
β	T [MeV]	STAT	$\text{Re}(L)$	$\langle \bar{\psi}\psi \rangle$
3.7600	200(29)	7760	$1.57(07) \cdot 10^{-3}$	0.05146(10)
3.7800	206(24)	3328	$1.80(10) \cdot 10^{-3}$	0.04769(15)
3.8000	212(20)	3097	$2.25(06) \cdot 10^{-3}$	0.04398(19)
3.8200	218(16)	3516	$2.60(10) \cdot 10^{-3}$	0.04091(17)
3.8400	225(13)	3279	$3.19(08) \cdot 10^{-3}$	0.03783(18)
3.8650	228(11)	3450	$4.80(08) \cdot 10^{-3}$	0.03364(19)
3.8700	234(9)	5900	$4.38(10) \cdot 10^{-3}$	0.03357(14)
3.8750	235(8)	3600	$4.49(10) \cdot 10^{-3}$	0.03351(18)
3.8800	237(7)	8759	$5.07(18) \cdot 10^{-3}$	0.03233(44)
3.8850	239(7)	6400	$4.91(11) \cdot 10^{-3}$	0.03222(40)
3.8900	241(6)	7789	$5.17(13) \cdot 10^{-3}$	0.03258(36)
3.8950	243(6)	4450	$5.52(12) \cdot 10^{-3}$	0.03143(24)
3.9000	244(5)	5973	$5.81(11) \cdot 10^{-3}$	0.03101(20)
3.9100	246(5)	7250	$5.70(12) \cdot 10^{-3}$	0.03085(39)
3.9300	250(5)	8050	$7.23(10) \cdot 10^{-3}$	0.02967(14)
3.9700	258(5)	7276	$8.42(13) \cdot 10^{-3}$	0.02465(07)
4.0500	274(5)	8716	$1.24(2) \cdot 10^{-2}$	0.02060(03)
4.1000	309(5)	1517	$1.44(3) \cdot 10^{-2}$	0.01873(04)
4.2000	333(9)	4131	$2.00(2) \cdot 10^{-2}$	0.01564(01)

TABLE V: Statistics for gauge observables from our simulations as well as expectation values of $\text{Re}(L)$ and $\langle \bar{\psi}\psi \rangle$. Note that the trajectory length differs between the runs. On the apeNEXT (B10, C12 except for $\beta = 4.06$) $\tau = 0.5$, on the HLRN (A12, B12, $\beta = 4.06$ of C12) $\tau = 1$.

- Tar, H. Ding, S. Gottlieb, R. Gupta, P. Hegde, H. U.M., and F. Karsch, *Phys.Rev.* **D85**, 054503 (2012), 1111.1710.
- [17] M. Creutz, *PoS Confinement8*, 016 (2008), 0810.4526.
- [18] O. Philipsen, *PoS CPOD2009*, 026 (2009), 0910.0785.
- [19] F. Karsch and E. Laermann, *Phys. Rev.* **D50**, 6954 (1994), hep-lat/9406008.
- [20] C. W. Bernard et al., *Phys. Rev. Lett.* **78**, 598 (1997), hep-lat/9611031.
- [21] Y. Iwasaki et al., *Phys. Rev. Lett.* **78**, 179 (1997), hep-lat/9609022.
- [22] S. Aoki et al. (JLQCD), *Phys. Rev.* **D57**, 3910 (1998), hep-lat/9710048.
- [23] A. Ali Khan et al. (CP-PACS), *Phys. Rev.* **D63**, 034502 (2001), hep-lat/0008011.
- [24] S. Ejiri et al., *Phys. Rev.* **D80**, 094505 (2009), 0909.5122.
- [25] M. D’Elia, A. Di Giacomo, and C. Pica, *Phys. Rev.* **D72**, 114510 (2005), hep-lat/0503030.
- [26] G. Cossu, M. D’Elia, A. Di Giacomo, and C. Pica (2007), 0706.4470.
- [27] C. Bonati et al., *PoS Lat2008*, 204 (2008), 0901.3231.
- [28] S. Aoki, H. Fukaya, and Y. Taniguchi (2012), 1209.2061.
- [29] C. Bonati, P. de Forcrand, M. D’Elia, O. Philipsen, and F. Sanfilippo, *PoS LATTICE2011*, 189 (2011), 1201.2769.
- [30] R. D. Pisarski and F. Wilczek, *Phys. Rev.* **D29**, 338 (1984).
- [31] A. Shindler, *Phys. Rept.* **461**, 37 (2008), 0707.4093.
- [32] T. Umeda et al., *Phys. Rev.* **D79**, 051501 (2009), 0809.2842.
- [33] V. Bornyakov, R. Horsley, Y. Nakamura, M. Polikarpov, P. Rakow, and G. Schierholz, *PoS Lat2010*, 170 (2011), 1102.4461.
- [34] B. Brandt, A. Francis, H. Meyer, O. Philipsen, and H. Wittig (2012), 1210.6972.
- [35] R. Baron et al. (ETM), *JHEP* **08**, 097 (2010), 0911.5061.
- [36] C. Urbach, K. Jansen, A. Shindler, and U. Wenger, *Comput.Phys.Commun.* **174**, 87 (2006), hep-lat/0506011.
- [37] K. Jansen and C. Urbach, *Comput.Phys.Commun.* **180**, 2717 (2009), 0905.3331.
- [38] E.-M. Ilgenfritz, K. Jansen, M. P. Lombardo, M. Müller-Preussker, M. Petschlies, O. Philipsen, and L. Zeidlewicz (tmfT Collaboration), *Phys.Rev.* **D80**, 094502 (2009), 0905.3112.
- [39] F. Burger, E.-M. Ilgenfritz, M. Kirchner, M. P. Lombardo, M. Müller-Preussker, O. Philipsen, C. Urbach, and L. Zeidlewicz (tmfT Collaboration), *PoS Lat2010*, 220 (2010), 1009.3758.
- [40] M. Müller-Preussker et al. (tmfT Collaboration), *PoS Lat2009*, 266 (2009), 0912.0919.
- [41] P. Dimopoulos, R. Frezzotti, C. Michael, G. C. Rossi, and C. Urbach, *Phys. Rev.* **D81**, 034509 (2010), 0908.0451.
- [42] Y. Aoki, Z. Fodor, S. Katz, and K. Szabo, *Phys.Lett.* **B643**, 46 (2006), hep-lat/0609068.
- [43] R. Sommer, *Nucl. Phys.* **B411**, 839 (1994), hep-lat/9310022.
- [44] C. DeTar (2011), to appear in Proceedings of the Kyoto Workshop on Thermal Quantum Field Theory and its Application, August 28-30, 2010, Soryushiron Kenkyu (Study of Particle Theory)., 1101.0208.
- [45] R. Frezzotti et al., *JHEP* **04**, 038 (2006), hep-lat/0503034.
- [46] S. Dinter et al. (ETM Collaboration), *JHEP* **1208**, 037 (2012), 1202.1480.
- [47] P. Boucaud et al. (ETM), *Comput. Phys. Commun.* **179**, 695 (2008), 0803.0224.
- [48] O. Philipsen and L. Zeidlewicz, *Phys. Rev.* **D81**, 077501 (2010), 0812.1177.
- [49] F. Karsch, *Phys. Rev. D* **49**, 3791 (1994).
- [50] V. G. Bornyakov et al., *Phys. Rev.* **D82**, 014504 (2010), 0910.2392.
- [51] M. E. Fisher and A. N. Berker, *Phys.Rev.* **B26**, 2507 (1982).
- [52] D. Toussaint, *Phys. Rev.* **D55**, 362 (1997), hep-lat/9607084.
- [53] J. Engels and T. Mendes, *Nucl. Phys.* **B572**, 289 (2000), hep-lat/9911028.
- [54] Y. Aoki et al., *JHEP* **06**, 088 (2009), 0903.4155.